An Integrated Rotary Transformer and 3-Phase Dual-Active-Bridge Converter for High Power Transfer in Novel X-rotor Wind Turbines

Reza Yazdanpanah[1], Seyed Abolfazl Mortazavizadeh[1], Yang Teng[1], Olimpo Anaya-Lara[1] and David Campos-Gaona[1]

[1]Department of Electronic and Electrical Engineering, University of Strathclyde, Glasgow, UK, d.campos-gaona@strath.ac.uk

The slip ring solution for power transfer between rotating structures has adverse impact the maintenance of offshore wind turbines. In this paper the design, performance, efficiency, and manufacturing details of a 1 MW wireless power transfer system for the novel X-rotor offshore wind turbine concept is presented. The results show that this design methodology that includes rotary transformers and dual active bridge converters is suitable for high-efficiency high-power wireless transfer systems.

***Index Terms*— dual active bridge, rotary transformer, wireless power transfer, X-rotor**

I. Introduction

Operation and Maintenance (O&M) of offshore wind turbines is, by far, the largest cost element of the levelized cost of energy (LCOE) of an offshore wind farm project [1]. The quest for reducing the LCOE has led to the recent deployment of the EU-funded X-rotor project [2]. The X-rotor is a novel hybrid wind turbine that retains some of the advantages of Vertical-Axis Wind Turbines [3]. A key feature of the X-rotor is the use of secondary rotors, mounted in a X-shaped vertical axis structure.

One requirement in the X-rotor operation is the capacity to transfer the power generated by secondary rotors from a rotating structure to the turbine tower. Given the well-documented impact of slip-rings in offshore wind turbine O&M [4], the necesity of MW-level wireless power transfer (WPT) arises to retain the advantages of the X-rotor system.

This research focuses in the magnetic design and finite element simulation/verification of a MW-level, medium-frequency Rotary Transformer (RT) interfaced by a 3-phase (3-hp) dual-active-bridge (DAB) converter for WPT.

The results of this research show an efficiency of 96.3% for a 1-MW RT and DAB system, which are among the highest reported in open literature. The design methodology and verification of this system are presented in the following sections of this paper.

II. Rotary Transformer

RTs are adopted to transfer energy from primary to secondary in situations in which the two sides are in relative rotation [5]. The structure of RT is shown in Fig. 1. The diameter D_{sh} of the cylindric structure supporting the primary winding of the RT is typically around 1.2m for a 5MW X-rotor system. The magnetic equivalent circuit (MEC) of the RT include the reluctances ($\Re$) and θ_1 and θ_2 which are windings' magneto-motive forces.

A. Design

The most important challenges in the electromagnetic design of the understudy RT comes from its geometrical size, power, and frequency as determined by the application. Therefore, the main contribution of this design approach is finding the solution while considering constraints.

Large inner and outer radiuses, and air-gap affect considerably the leakage inductance and coupling factor, so the MEC is used for proper dimensioning of the RT to have low leakage and high coupling performance.

Mechanical and thermal considerations are included for selecting constants of Table I, which have values different from conventional power transformers.

The behavior of a transformer can significantly change as frequency increases, hence, in this medium frequency RT, the skin effect and proximity effect are included as the parasitic effects on the windings.

Based on efficiency needs, the design approach uses low loss, low flux density core for high power high efficiency RT.

To design a RT, first the MEC should be used to calculate the winding number of turns for producing a specific flux density in the air-gap (B_g). Then, Faraday's Law relates volts–amp products for each winding to the core and coil dimensions as:

$$\sum VA = KfBA_cA_wJk_{cu}k_c \qquad (1)$$

where k_{cu}, k_c are the winding fill factor and lamination fill factor, respectively. A_w and A_c are the core and winding cross sectional area and J is the current density.

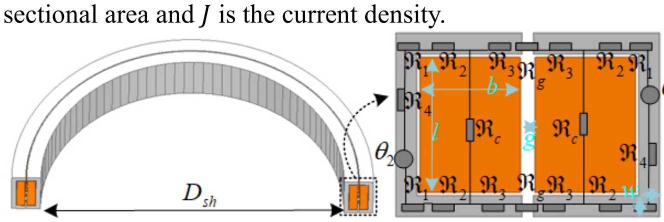

Fig. 1. RT structure and MEC

Above sizing equation and MEC help to calculate main geometrical parameters such as winding and core cross sectional areas, core thickness, and number of turns based on the initial parameters of the RT shown in Table I. By having the geometrical and electromagnetic parameters, one can calculate the electrical model parameters including the resistances and inductances using geometry and the MEC. Finally, the core and copper losses can be estimated by the Steinmetz's equation and resistances dissipation power.

Table I: Preliminary parameters

Parameter	Value	Parameter	Value
RMS voltage (V)	850	current density (A/mm^2)	2
frequency (Hz)	2000	lamination fill factor	0.85
flux density (T)	0.50	shaft radius (mm)	650
Power (MVA)	1/3	air-gap length (mm)	5.00
winding fill factor	0.30	fringing-effect factor	1.10

By using the design equations and preliminary parameters, and considering a nanocrystalline and ferrite core, the RT was designed with the resulting parameters shown in Table II.

This is a peer-reviewed, accepted author manuscript of the following paper: Yazdanpanah, R., Mortazavizadeh, S. A., Teng, Y., Anaya-Lara, O., & Campos-Gaona, D. (Accepted/In press). An integrated rotary transformer and 3-phase dual-active-bridge converter for high power transfer in novel X-rotor wind turbines. In IEEE International Magnetics Conference: INTERMAG2023 IEEE.

Table II. Designed RT parameters

Parameter	Value	Parameter	Value
RMS current (A)	392	b (mm)	40
cond. x-sec. (mm^2)	196	number of turns N	10
Aw (mm^2)	6635	prim. wind. res. $R_{in,ac}$ (ohm)	0.0113
Ac (mm^2)	22162	sec. wind. res. $R_{out,ac}$ (ohm)	0.0120
w (mm)	20	mutual ind. M (mH)	2.43
l (mm)	166	leak. inductances L_{11}, L_{22} (mH)	0.06

A series parallel (SP) compensation topology [6] is used to improve the input-power-factor with 53&2.5 µF capacitances.

B. Results

To show the electromagnetic performance of the designed RT, 3D numerical simulation was performed. Voltage and current for the output power of 316 kW (i.e. one phase of the system) is shown in Fig. 2, that are in good accordance with analytical results as well as the desired high power factor in the input.

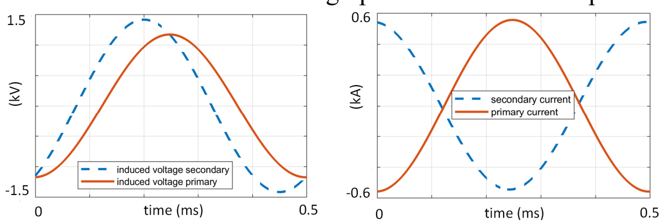

Fig. 2: FEA simulation, voltage and current, 333 kVA

Based on the FEA calculated losses, a heat transfer analysis was done for the ambient temperature and the equivalent heat transfer coefficient of 40 °C and 30 W/m^2 °C, respectively.

Fig. 3 shows the magnetic flux density and the temperature distribution in RT that illustrates no saturation in the core. Finally, the analytical and numerical results are compared in *Table III* to validate the design procedure of the RT.

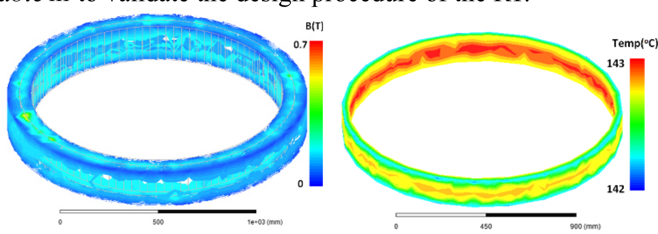

Fig. 3: Magnetic flux and temperature distribution, 333 kVA

Table III: Design validation

Parameter	Analytical	FEA
Leakage inductance (mH)	0.053	0.06
Magnetizing inductance (mH)	2.1	2.43
Core loss (kW)	1.52	1.44
Copper loss (kW)	3.5	3.45

III. INTEGRATED RT AND DAB CONVERTER

A. DAB Converter

3-ph DAB converters offer reduced current magnitude, sinusoidal current waveforms, reduced harmonic components, lower losses, and lower ripples in output voltage [7].

In this research two 3-ph DAB are connected to each other through inductors and three 1-ph RTs using a YY connection. The angle difference between primary and secondary voltage ϕ generated by the primary and secondary DAB defines the direction and magnitude of power transfer between windings. The switching frequency is fixed to 2 kHz with an output capacitor chosen to keep the output voltage under 5% ripple.

B. Simulation of 1MW wireless power transfer system

The DAB and RT system was simulated in MATLAB/Simulink along with its compensation network. Both electrical and thermal performance analysis were undertaken. Fig. 4 shows the voltage and current of one phase of the RT when 1 MW power transfer from primary to secondary occurs. The target power output of 1MW is achieved at when $\phi = 30°$. The input and output voltages change are in the allowed ranges that are less than 5%.

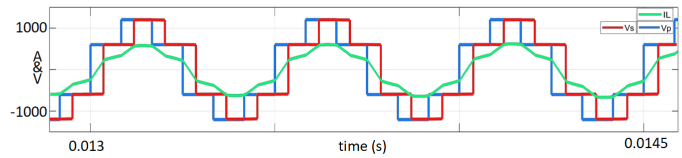

Fig. 4. The RT's primary (Vp) and secondary (Vs) voltage, primary current (IL)

Thermal analysis results are presented in Fig. 5 by considering 40 °C for the ambient temperature.

Based on the simulation results, the power electronics losses were calculated as 23 kW, for 1 MW power transfer. Moreover, the RTs core and copper losses are 14.67 kW. As such, the total efficiency of the wireless power transfer system is calculated to be 96.3%. Here it is important to highlight that his efficiency results do not rely on unconventional manufacture elements or practices.

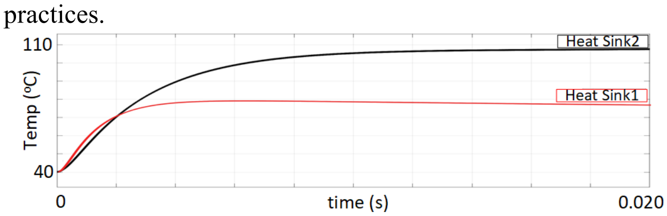

Fig. 5. Temperature rise in the input and output heat sinks of the DABs

CONCLUSION

In this article, a WPT system for a novel wind turbine concept has been designed and analyzed based on magnetic field calculation, and electric circuit analysis. Simulation results verify the design methodology, which can generate high-power, high-efficiency WPT using conventional manufacturing elements and practices.

REFERENCES

[1] P. B. Tyler Stehly, Patrick Duffy, "2019 Cost of Wind Energy Review," NREL, 2020. Available: https://www.nrel.gov/docs/fy21osti/78471.pdf.

[2] Horizon-2020. "X-ROTOR: X-shaped Radical Offshore wind Turbine for Overall cost of energy Reduction." European Comission. https://cordis.europa.eu/project/id/101007135 (accessed 2022).

[3] C. Flannigan, J. Carroll, and W. Leithead, "Operations expenditure modelling of the X-Rotor offshore wind turbine concept," *Journal of Physics: Conference Series,* vol. 2265, no. 3, pp. 032054, 2022.

[4] J. Carroll, A. McDonald, and D. McMillan, "Failure rate, repair time and unscheduled O&M cost analysis of offshore wind turbines," *Wind Energy,* vol. 19, no. 6, pp. 1107-1119, 2016.

[5] T. Raminosoa, R. H. Wiles, and J. Wilkins, "Novel Rotary Transformer Topology With Improved Power Transfer Capability for High-Speed Applications," *IEEE Transactions on Industry Applications,* vol. 56, no.1, pp. 277-286, 2020.

[6] B. D. Truong, C. Roundy, E. Andersen, and S. Roundy, "Analysis of Resonance and Anti-Resonance Frequencies in a Wireless Power Transfer System: Analytical Model and Experiments," *IEEE Transactions on Circuits and SystemsII:Express Briefs,* vol. 66, no. 7, pp. 1222-1226, 2019.

[7] D. D. Nguyen, N. T. Bui, and K. Yukita, "Design and Optimization of Three-Phase Dual-Active-Bridge Converters for Electric Vehicle Charging Stations," *Energies,* vol. 13, no. 1, pp. 150, 2020.